J Intell Robot Syst (2012) 65:389–408
DOI 10.1007/s10846-011-9583-3

Comparative Results on Stabilization of the Quad-rotor Rotorcraft Using Bounded Feedback Controllers

Nikola Georgiev Shakev · Andon Venelinov Topalov · Okyay Kaynak · Kostadin Borisov Shiev

Received: 15 February 2011 / Accepted: 18 April 2011 / Published online: 16 August 2011

Abstract In the recent years autonomous flying vehicles are being increasingly used in both civil and military areas. With the advancement of the technology it has become possible to test efficiently and cost-effectively different autonomous flight control concepts and design variations using small-scale aerial vehicles. In this paper the stabilization problem of the quad-rotor rotorcraft using bounded feedback controllers is investigated. Five different types of nonlinear feedback laws with saturation elements, previously proposed for global control of systems with multiple integrators, are applied and tested to control the quad-rotor rotorcraft roll and pitch angles. The results obtained from autonomous flight simulations and real time experiments with the Draganflyer V Ti four-rotor mini-rotorcraft are analyzed with respect to the structural simplicity of the control schemes and the transient performance of the closed-loop system.

Keywords Unmanned aerial vehicles · Quad-rotor rotorcraft · Nonlinear control · Stabilization

N. G. Shakev · A. V. Topalov (✉) · K. B. Shiev
Control Systems Department,
Technical University—Sofia, campus Plovdiv,
25 Tsanko Dustabanov Str, 4000 Plovdiv, Bulgaria
e-mail: topalov@tu-plovdiv.bg

N. G. Shakev
e-mail: shakev@tu-plovdiv.bg

K. B. Shiev
e-mail: k.shiev@gmail.com

O. Kaynak
Department of Electrical and Electronic Engineering,
Bogazici University, 34342 Bebek, Instanbul, Turkey
e-mail: okyay.kaynak@boun.edu.tr

1 Introduction

Unmanned helicopters are versatile aerial vehicles designed to operate with high agility since they are required, in many applications, to perform aggressive maneuvers, and work in degraded environments including wind gusts etc. Autonomous flight control of helicopters is therefore an area that imposes challenging problems for control researchers.

The quad-rotor aerial vehicles offer a suitable, more tractable, case study for the control of rotorcraft. In comparison with the control of classical helicopters the quad-rotor control design is quite similar and can be implemented easily. Therefore, different control techniques for quad-rotor aerial vehicles have been proposed and investigated in the literature. Among the popular methods are linearization and linear quadratic

regulator (LQR) [1, 2], H-infinity state-space design and feedback linearization [3, 4], model-predictive control [5], and backstepping [6]. On-line tuned neural networks using adaptive control techniques are frequently implemented for handling unknown nonlinearities [6, 7].

The DraganFlyer V Ti four-rotor mini-rotorcraft is an excellent flying vehicle test bed allowing researchers to investigate efficiently and cost-effectively different autonomous flight control concepts and design issues. It has an empty weight of 482 g and can carry a payload of up to 300 g (see Fig. 1). Its flight endurance is about 12–15 min. The airframe consists of four carbon fiber arms attached to a central platform which houses the electronics and the battery. Each rotor is situated at the end of one of the arms and is composed of two blades. The quad-rotor electronic circuit board has three gyros, four pulse-width modulation speed controllers and a microprocessor that mixes the received commands to calculate the necessary rotor control inputs. The gyro stabilization serves to introduce damping into the system in order to simplify the manual control.

Small aerial vehicles impose some restrictions that have to be considered in the design of the control law. In particular, saturation nonlinearities are prevalent and actuator saturation has a significant effect on the overall stability of the aircraft [8].

For linear systems subject to input saturation, several important control problems, such as global stabilization [9, 10], semi-global stabilization [11], local stabilization [12, 13], input–output stabilization [14] and robust stabilization [15] have already been solved. In the special case of systems with multiple integrators a nonlinear state feedback law consisting of nested saturation functions has been proposed by Teel to solve the global stabilization problem [16]. It can also be used to achieve trajectory tracking for a class of bounded trajectories. The technique of using nested saturation functions has recently been applied by Castillo et al., [2, 17, 18] to control a planar vertical take-off and landing (PVTOL) aircraft and to achieve stabilization of a quad-rotor mini-rotorcraft.

It is shown in [19] that Teel's feedback law consisting of n (the order of the system) nested saturation functions exhibits good robustness and excellent disturbance rejection, and is noticeably superior to some other existing feedback laws. On the other hand, it has been observed that for larger systems and larger initial conditions, the transient performance of the closed-loop system is degraded, [20] and that the Teel's nonlinear feedback laws result in all poles of the closed-loop system to reside at -1 when none of the saturation elements in the control laws is saturated [21, 22]. Due to its simplicity, the approach attracted a

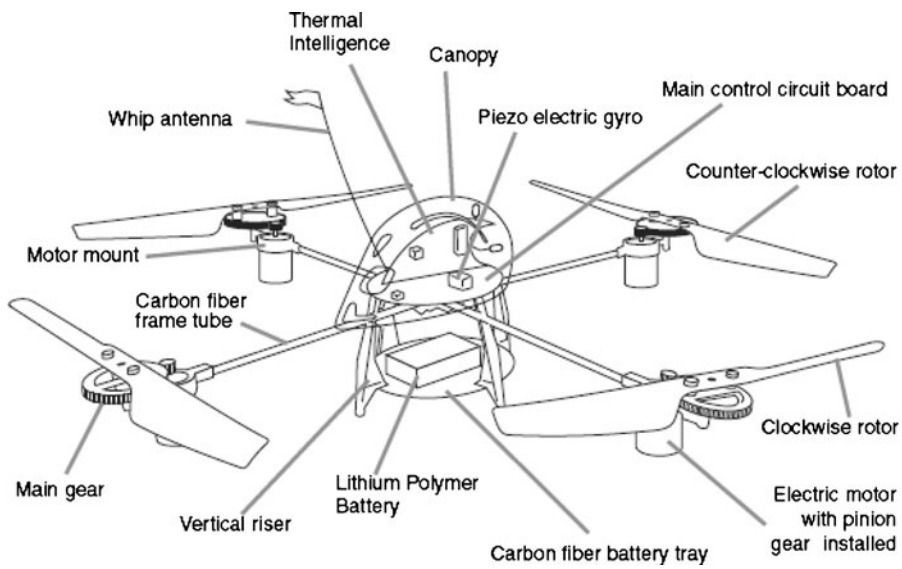

Fig. 1 The DraganFlyer V Ti miniature aerial vehicle

lot of attention and a number of modifications have been offered (see, e.g., [20–28]) in order to improve the transient response at bigger initial conditions and to allow the poles of the closed-loop system to reside at any location of the negative real axis when none of the saturation elements in the control laws is saturated.

Hably et al. [29] has exploited the control technique in [23] to achieve global stabilization of the PVTOL aircraft and has shown that the controller presents good performance (convergence speed) as compared to the approaches presented earlier in [17]. The same authors have proposed in [30] a control law for the global stabilization of a four-rotor helicopter with bounded inputs, based on the results presented in [9] and [28]. Their work can be also seen as a generalization of the previous result obtained in [29].

In this paper an approximation of the simplified quad-rotor rotorcraft dynamics to four integrators in cascade is proposed. To make this possible the dynamic model is considered with respect to a reference frame attached to the aerial vehicle. Five nonlinear feedback control laws with saturation elements, initially proposed in [16, 22, 23] for the global stabilization of a chain of integrators, are implemented to control the pitch and roll angles, and X, Y displacements of the quad-rotor rotorcraft. Their performance is compared based on a number of autonomous flight simulations experiments using a precise dynamical model of the DraganFlyer V Ti four-rotor rotorcraft. The obtained results are analyzed with respect to the structural simplicity of the control scheme and the transient performance of the closed-loop system. The control law showing the best performance in simulations is then tested in real-time autonomous flight experiments.

2 Stabilization of the Quad-rotor Rotorcraft with Bounded Controls

2.1 Simplified Dynamics of the Quad-rotor Rotorcraft

For the description of the quad-rotor rotorcraft motion two frames have to be used: an inertial earth frame $\{R_E\}$ (I,X,Y,Z) and a frame fixed to the center of mass of the aerial vehicle $\{R_B\}$ (G,x,y,z). The relation between the frame $\{R_B\}$ and the frame $\{R_E\}$ can be obtained by the position vector $\xi = (X, Y, Z)^T \in \Re^3$, which describes the displacement of the center of mass G in the inertial frame and the orientation vector $\eta = (\psi, \theta, \phi)^T \in \Re^3$ where (ψ, θ, ϕ) are the three Euler angles (yaw, pitch, and roll) representing the orientation (Fig. 1).

The generalized coordinates for the rotorcraft are

$$q = (X, Y, Z, \psi, \theta, \phi)^T \in \Re^6 \tag{1}$$

The dynamic model of the rotorcraft can be developed using the Lagrangian form of the dynamics [2, 17, 18]. A simplified model can be obtained by representing the quad-rotor rotorcraft as a solid body evolving in 3D space and subject to one force and three moments (Fig. 2).

The translational kinetic energy of the rotorcraft can be described as

$$T_{trans} = \frac{1}{2} m \dot{\xi}^T \dot{\xi} \tag{2}$$

where m is the mass of rotorcraft.

The rotational kinetic energy is given by

$$T_{rot} = \frac{1}{2} \dot{\eta}^T J \dot{\eta} \tag{3}$$

where $J = diag\left(I_{xx}, I_{yy}, I_{zz}\right)$ is the inertia matrix expressed in terms of the coordinates η.

The only potential energy that needs to be considered is caused by the gravitational force

$$U = mgZ \tag{4}$$

In such a case the Lagrangian is given by

$$\mathcal{L}(q, \dot{q}) = T_{trans} + T_{rot} - U \tag{5}$$

$$\mathcal{L}(q, \dot{q}) = \frac{1}{2} m \dot{\xi}^T \dot{\xi} + \frac{1}{2} \dot{\eta}^T J \dot{\eta} - mgZ \tag{6}$$

Then the model for the quad-rotor helicopter dynamics can be deduced by using the Lagrange-Euler equations with external generalized force

$$\frac{d}{dt} \frac{\partial \mathcal{L}}{\partial \dot{q}} - \frac{\partial \mathcal{L}}{\partial q} = F \tag{7}$$

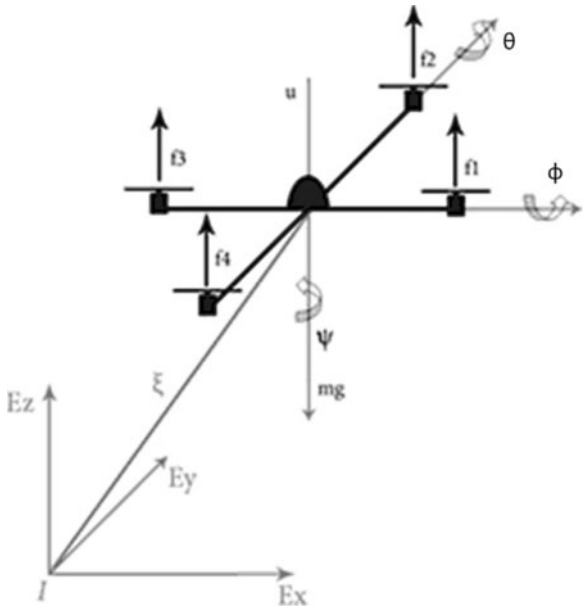

Fig. 2 Schema of the four-rotor rotorcraft

where $F = (F_\xi, \tau)$. F_ξ defines the translational force applied to the rotorcraft due to the control inputs and relative to the frame $\{R_E\}$, and τ is the generalized moments vector. In the simplified dynamic model the small body forces are ignored because of their smaller magnitude and only the principal control inputs u and τ are considered, where u represents the total thrust, and τ is the generalized moment.

Each propeller generates vertical lifting force, denoted as f_1, f_2, f_3, f_4 respectively and

$$f_i = k\omega_i^2 \quad (i = 1, 2, 3, 4) \tag{8}$$

where ω_i is the rotational speed of the propeller and k is a positive constant. Supposing the forces are parallel, the overall lifting force will act along the axes Gz in $\{R_B\}$ frame, and its magnitude will be:

$$u = f_1 + f_2 + f_3 + f_4 \tag{9}$$

Then the force applied to the mini-rotorcraft relative to frame $\{R_B\}$ is defined as

$$F_B = [0 \quad 0 \quad u]^T \tag{10}$$

For Z–Y–X Euler angles the transition between F_B and F_ξ can be done by the rotational matrix R [31].

$$R = \begin{bmatrix} C_\theta C_\psi & C_\psi S_\theta S_\phi - C_\phi S_\psi & C_\phi C_\psi S_\theta + S_\phi S_\psi \\ C_\theta S_\psi & S_\theta S_\phi S_\psi + C_\phi C_\psi & C_\phi S_\theta S_\psi - C_\psi S_\phi \\ -S_\theta & C_\theta S_\phi & C_\theta C_\phi \end{bmatrix} \tag{11}$$

where $S_{(\cdot)}$ and $C_{(\cdot)}$ represent $\sin(\cdot)$ and $\cos(\cdot)$ respectively. Then

$$F_\xi = RF_B \tag{12}$$

$$F_B = R^T F_\xi \tag{13}$$

The generalized moments on the η variables are

$$\tau = \begin{bmatrix} \tau_\phi \\ \tau_\theta \\ \tau_\psi \end{bmatrix} = \begin{bmatrix} (f_4 - f_2)\, l \\ (f_3 - f_1)\, l \\ \left(\omega_2^2 + \omega_4^2 - \omega_1^2 - \omega_3^2\right) d \end{bmatrix} \tag{14}$$

where l denotes the distance from any motor to the center of mass and d is a drag constant.

Therefore the Lagrange–Euler equations can be rewritten as

$$m\ddot{\xi} + \begin{bmatrix} 0 \\ 0 \\ mg \end{bmatrix} = F_\xi \tag{15}$$

$$J\ddot{\eta} + \dot{J}\dot{\eta} - \frac{1}{2}\frac{\partial}{\partial \eta}\left(\dot{\eta}^T J \dot{\eta}\right) = \tau \tag{16}$$

Defining the Coriolis/centripetal vector as

$$F_c(\eta, \dot{\eta}) = \dot{J} - \frac{1}{2}\frac{\partial}{\partial \eta}\left(\dot{\eta}^T J\right) \tag{17}$$

the expression 16 can be rewritten as

$$J(\eta)\,\ddot{\eta} + F_c(\eta, \dot{\eta})\,\dot{\eta} = \tau \tag{18}$$

Finally, the equations of motion for the four-rotor rotorcraft are expressed as

$$m\ddot{\xi} = F_\xi + \begin{bmatrix} 0 \\ 0 \\ -mg \end{bmatrix} \tag{19}$$

$$J\ddot{\eta} = \tau - F_c(\eta, \dot{\eta})\,\dot{\eta} \tag{20}$$

Since J is nonsingular, it is possible to simplify the analysis changing the input variable as follows

$$\tau = J\tilde{\tau} + F_c(\eta, \dot{\eta})\,\dot{\eta} \tag{21}$$

where

$$\tilde{\tau} = \begin{bmatrix} \tilde{\tau}_\phi & \tilde{\tau}_\theta & \tilde{\tau}_\psi \end{bmatrix}^T \tag{22}$$

are the new inputs. Then it follows that

$$\ddot{\eta} = \tilde{\tau} \tag{23}$$

Finally we obtain from Eqs. 12, 19 and 23:

$$m\ddot{X} = u\left(C_\phi C_\psi S_\theta + S_\phi S_\psi\right), \tag{24}$$

$$m\ddot{Y} = u\left(C_\phi S_\theta S_\psi - C_\psi S_\phi\right), \tag{25}$$

$$m\ddot{Z} = uC_\phi C_\theta - mg, \tag{26}$$

$$\ddot{\psi} = \tilde{\tau}_\psi, \tag{27}$$

$$\ddot{\theta} = \tilde{\tau}_\theta, \tag{28}$$

$$\ddot{\phi} = \tilde{\tau}_\phi \tag{29}$$

In the dynamical model 24–29 the total trust $u \in \Re$ and torque $\tilde{\tau} \in \Re^3$ are the control inputs, consequently it is a coupled Lagrangian form underactuated system with six outputs and four inputs.

2.2 Altitude and Yaw Control Law Formulation

Since the quad-rotor rotorcraft is dynamically unstable, control algorithms are required for stabilization.

The vertical displacement Z in Eq. 26 can be controlled by forcing the altitude to satisfy the dynamics of a linear system. Therefore the total trust is set [2, 17, 18]:

$$u = (r_1 + mg)\frac{1}{\cos\phi\cos\theta}, \tag{30}$$

where r_1 is a term that is calculated in accordance with the proportional plus derivative (PD) control law

$$r_1 = -a_{z1}\left(\dot{Z} - \dot{Z}_d\right) - a_{z2}\left(Z - Z_d\right), \tag{31}$$

where Z_d is the desired altitude.

The yaw angular position can be controlled by applying also a PD control law

$$\tilde{\tau}_\psi = -a_{\psi 1}\left(\dot{\psi} - \dot{\psi}_d\right) - a_{\psi 2}\left(\psi - \psi_d\right), \tag{32}$$

where ψ_d is the desired yaw angle.

Introducing Eqs. 30–32 into Eqs. 24–27 and assuming $\cos\theta\cos\phi \neq 0$, that is, $\theta,\ \phi \in (-\pi/2, \pi/2)$ it can be obtained that

$$m\ddot{X} = (r_1 + mg)\left(C_\phi C_\psi S_\theta + S_\phi S_\psi\right)/\left(C_\phi C_\theta\right) \tag{33}$$

$$m\ddot{Y} = (r_1 + mg)\left(C_\phi S_\theta S_\psi - C_\psi S_\phi\right)/C_\phi C_\theta \tag{34}$$

$$m\ddot{Z} = \left[-a_{z1}\left(\dot{Z} - \dot{Z}_d\right) - a_{z2}\left(Z - Z_d\right)\right] \tag{35}$$

$$\ddot{\psi} = -a_{\psi 1}\left(\dot{\psi} - \dot{\psi}_d\right) - a_{\psi 2}\left(\psi - \psi_d\right) \tag{36}$$

The control gains $\alpha_{\psi 1}$, $\alpha_{\psi 2}$, α_{z1}, α_{z2} are positive constants that have to be chosen to ensure stable, well damped response of the quad-rotor helicopter in the vertical and yaw axes.

From Eqs. 35 and 36 it follows that, if ψ_d and z_d are constants, then ψ and z converge. Therefore, $\dot{\psi}$ and $\ddot{\psi} \to 0$, which, using Eq. 36, implies that $\psi \to \psi_d$. Similarly, $z \to z_d$. It has to be noted that from Eqs. 31 and 35 it follows that $r_1 \to 0$.

2.3 Pitch and Roll Control Strategy

The main task of the pitch and roll control channels is to ensure stabilization of the pitch and roll angles respectively. In addition since the system is underactuated and the pitch and roll dynamics are both coupled with X and Y displacements (see Eqs. 33 and 34) they can be considered also as control inputs for both X and Y channels.

In order to reduce the dynamics coupling it is useful to design the control law with respect to $\{R_B\}$. Thus the acceleration vector can be represented as follows

$$m\begin{bmatrix} \ddot{x} \\ \ddot{y} \\ \ddot{z} \end{bmatrix} = mR^T\begin{bmatrix} \ddot{X} \\ \ddot{Y} \\ \ddot{Z} \end{bmatrix} = R^T\begin{bmatrix} m\ddot{X} \\ m\ddot{Y} \\ m\ddot{Z} \end{bmatrix} \tag{37}$$

Substituting Eqs. 11, 24–26 and 30 in Eq. 37 one can obtain

$$m\ddot{x} = mg\sin(\theta) \tag{38}$$

$$m\ddot{y} = -mg\sin(\phi)\cos(\theta) \tag{39}$$

To implement the pitch control strategy we will consider the subsystem given by Eqs. 28 and 38.

The roll and pitch angles ϕ, θ theoretically are limited to $\pm\pi/2$, but in fact they take smaller values since the upper lift, which compensates the gravity typically is much greater than the forces producing horizontal movement during the flight. To further simplify the analysis we will impose an upper bound on $|\phi|$ and $|\theta|$ in such a way that the difference $\sin(\theta) - \theta$ is arbitrarily small. Therefore the subsystem 28 and 38 reduces to

$$\ddot{x} = g\theta \tag{40}$$

$$\ddot{\theta} = \tilde{\tau}_\theta \tag{41}$$

which represents four integrators in cascade.

Let us denote the state vector χ_θ

$$\chi_\theta = \begin{bmatrix} \chi_{\theta 1} & \chi_{\theta 2} & \chi_{\theta 3} & \chi_{\theta 4} \end{bmatrix}^T = \begin{bmatrix} x/g & \dot{x}/g & \theta & \dot{\theta} \end{bmatrix}^T; \tag{42}$$

$$\dot{\chi}_\theta = \begin{bmatrix} \dot{\chi}_{\theta 1} & \dot{\chi}_{\theta 2} & \dot{\chi}_{\theta 3} & \dot{\chi}_{\theta 4} \end{bmatrix}^T = \begin{bmatrix} \chi_{\theta 2} & \chi_{\theta 3} & \chi_{\theta 4} & \tilde{\tau}_\theta \end{bmatrix}^T; \tag{43}$$

If we choose a series of positive numbers $\lambda_2, \lambda_3, \lambda_4$ then Eq. 43 is equivalent to

$$\dot{P} = AP + b\tilde{\tau} \tag{44}$$

where A and b are respectively

$$A = \begin{bmatrix} 0 & \lambda_2 & \lambda_3 & \lambda_4 \\ 0 & 0 & \lambda_3 & \lambda_4 \\ 0 & 0 & 0 & \lambda_4 \\ 0 & 0 & 0 & 0 \end{bmatrix}, b = \begin{bmatrix} 1 \\ 1 \\ 1 \\ 1 \end{bmatrix}, \tag{45}$$

and the following linear change of coordinates is used

$$P = T\chi. \tag{46}$$

The matrix T is

$$T = \begin{bmatrix} A^3 b & A^2 b & Ab & b \end{bmatrix} \tag{47}$$

The control laws for the stabilization of four integrators in cascade have the following general form:

$$\tilde{\tau}_\theta = \tilde{\tau}_\theta(p_1, p_2, p_3, p_4) \tag{48}$$

From Eqs. 40, 41 and 48 we will obtain the pitch angle stabilization $\theta \to 0$, and then the dynamic subsystem 29, Eq. 39 becomes

$$\ddot{y} = -g\sin(\phi) \tag{49}$$

$$\ddot{\phi} = \tilde{\tau}_\phi \tag{50}$$

Here we also assume an upper bound of $|\phi|$ in such a way that $\sin(\phi) \approx \phi$. Then Eq. 49 reduces to

$$\ddot{y} = -g\phi \tag{51}$$

The state vector χ_ϕ can be defined as

$$\chi_\phi = \begin{bmatrix} \chi_{\phi 1} & \chi_{\phi 2} & \chi_{\phi 3} & \chi_{\phi 4} \end{bmatrix}^T = \begin{bmatrix} -y/g & -\dot{y}/g & \phi & \dot{\phi} \end{bmatrix}^T; \tag{52}$$

$$\dot{\chi}_\phi = \begin{bmatrix} \dot{\chi}_{\phi 1} & \dot{\chi}_{\phi 2} & \dot{\chi}_{\phi 3} & \dot{\chi}_{\phi 4} \end{bmatrix}^T = \begin{bmatrix} \chi_{\phi 2} & \chi_{\phi 3} & \chi_{\phi 4} & \tilde{\tau}_\phi \end{bmatrix}^T; \tag{53}$$

In a similar way, using the appropriate linear transformations 44–47, the general form of the control input $\tilde{\tau}_\phi$ can be obtained.

$$\tilde{\tau}_\phi = \tilde{\tau}_\phi(p_1, p_2, p_3, p_4) \tag{54}$$

3 The Compared Control Laws

Five different types of nonlinear feedback laws with saturation elements, initially proposed for global control of systems with multiple integrators, are applied in this investigation to control the DraganFlyer V Ti quad-rotor rotorcraft roll and pitch angles. They are compared with respect to the structural simplicity of the resulting control schemes and the transient performance of the closed-loop system.

Control Law 1 The Teel's first nonlinear feedback law with nested saturation functions [16] has been proposed for the stabilization of multiple integrators and can be presented in the following form

$$\tilde{\tau} = -\sigma_{\alpha 1}(p_4 + \sigma_{\alpha 2}(p_3 + \sigma_{\alpha 3}(p_2 + \sigma_{\alpha 4}(p_1)))) \tag{55}$$

where $\sigma_{\alpha i}(\cdot)$ is a saturation function defined as follows

$$\begin{aligned} &\sigma_{\alpha i}(s) = -\alpha_i \quad \text{if } s < -\alpha_i \\ &\sigma_{\alpha i}(s) = s \quad \text{if } -\alpha_i \le s \le \alpha_i \\ &\sigma_{\alpha i}(s) = \alpha_i \quad \text{if } s > \alpha_i \end{aligned} \tag{56}$$

To ensure the system stability, the saturation limits have to satisfy the inequality

$$\alpha_1 \ge 2\alpha_2 \ge 4\alpha_3 \ge 8\alpha_4. \tag{57}$$

In order to obtain the control laws for rotorcraft pitch and roll angles, the variables p_1,p_2, p_3, and p_4, have to be calculated separately for pitch and roll control channels using state vectors χ_θ and χ_ϕ respectively. Applying Eqs. 45–47 and considering $\lambda_i = 1$, i = 1,2,3,4 we achieve vector P and the following control laws respectively:

$$P\left(\theta,\dot{\theta},x,\dot{x}\right)=\begin{bmatrix}p_1\\p_2\\p_3\\p_4\end{bmatrix}=\begin{bmatrix}\dot{\theta}+3\theta+3\frac{\dot{x}}{g}+\frac{x}{g}\\2\theta+\dot{\theta}+\frac{\dot{x}}{g}\\\theta+\dot{\theta}\\\dot{\theta}\end{bmatrix} \tag{58}$$

$$P\left(\phi,\dot{\phi},y,\dot{y}\right)=\begin{bmatrix}p_1\\p_2\\p_3\\p_4\end{bmatrix}=\begin{bmatrix}\dot{\phi}+3\phi-3\frac{\dot{y}}{g}-\frac{y}{g}\\2\phi+\dot{\phi}-\frac{\dot{y}}{g}\\\phi+\dot{\phi}\\\dot{\phi}\end{bmatrix} \tag{59}$$

$$\tilde{\tau}_\theta=-\sigma_{\alpha1}\left(\dot{\theta}+\sigma_{\alpha2}\left(\theta+\dot{\theta}+\sigma_{\alpha3}\left(2\theta+\dot{\theta}+\frac{\dot{x}}{g}+\sigma_{\alpha4}\left(\dot{\theta}+3\theta+3\frac{\dot{x}}{g}+\frac{x}{g}\right)\right)\right)\right) \tag{60}$$

$$\tilde{\tau}_\phi=-\sigma_{\alpha1}\left(\dot{\phi}+\sigma_{\alpha2}\left(\phi+\dot{\phi}+\sigma_{\alpha3}\left(2\phi+\dot{\phi}-\frac{\dot{y}}{g}+\sigma_{\alpha4}\left(\dot{\phi}+3\phi-3\frac{\dot{y}}{g}-\frac{y}{g}\right)\right)\right)\right) \tag{61}$$

Since the five different control laws have to be compared it has been chosen $\tilde{\tau}_{\max}=\alpha_1=2$. In that way α_2, α_3, α_4 remain tunable parameters and we have achieved good results by selecting $\alpha_2=1,\ \alpha_3=0.2,\ \alpha_4=0.1$.

Remark 1 It is worth to be noted that the first attempt to apply the Teel's first nonlinear feedback law with saturation elements [16] to the quad-rotor rotorcraft pitch and roll control has been made in [2, 17, 18]. Unfortunately the authors have inappropriately operated with the rotation matrix [11] which has consequently led to an incorrect dynamical model of the aerial vehicle. Based on that incorrect model it has appeared possible to apply the nested saturations control strategy with respect to the inertial frame $\{R_E\}$ though this is inapplicable for the correct rotorcraft model described with the Eqs. 24–29. To the best of our knowledge the proposed approach in this paper implements for the first time correctly the Teel's first nonlinear feedback law with saturation elements to the quad-rotor rotorcraft pitch and roll control by carrying the control design with respect to a frame attached to the center of mass of the rotorcraft $\{R_B\}$.

In the Teel's original paper [16], actually two types of feedback laws consisting of nested saturation functions are proposed. Suppose n is the order of the system (the length of the multiple integrators), the first one consists of n saturation functions (four in the case of the quad-rotor rotorcraft stabilization) and the other needs only $\tilde{n}$ ($\tilde{n}=\frac{n}{2}$ if n is even and $\tilde{n}=\frac{n+1}{2}$if n is odd) saturation functions with the number significantly decreased. The existing in the literature discussions and modifications are mostly based on the Teel's first type of nested nonlinear feedback law while the other one is rarely mentioned. However, the second type of nonlinear feedback law is inherently superior to the first as it requires fewer saturation elements which can increase the control energy.

Control Law 2 The Teel's second control law has the form

$$\tilde{\tau}=-\alpha_2\sigma_1\left(\left(\frac{p_4+p_3}{\alpha_2}\right)+\frac{\alpha_1}{\alpha_2}\sigma_1\left(\frac{p_2+p_1}{\alpha_1}\right)\right) \tag{62}$$

where P is as in Eqs. 58 and 59 respectively. Substituting Eqs. 58 and 59 in Eq. 62 we obtain the control input for pitch and roll subsystems

$$\tilde{\tau}_\theta=-\alpha_2\sigma_1\left(\left(\frac{\theta+2\dot{\theta}}{\alpha_2}\right)+\frac{\alpha_1}{\alpha_2}\sigma_1\left(\frac{2\dot{\theta}+5\theta+4\frac{\dot{x}}{g}+\frac{x}{g}}{\alpha_1}\right)\right); \tag{63}$$

$$\tilde{\tau}_\phi=-\alpha_2\sigma_1\left(\left(\frac{\phi+2\dot{\phi}}{\alpha_2}\right)+\frac{\alpha_1}{\alpha_2}\sigma_1\left(\frac{2\dot{\phi}+5\phi-4\frac{\dot{y}}{g}-\frac{y}{g}}{\alpha_1}\right)\right), \tag{64}$$

where σ_1 is a function with saturation levels -1 and 1, and the values for parameters α_1 and α_2 are chosen as follows: $\alpha_2 = 2 = \tilde{\tau}_{\max}$; $\alpha_1 = 0.4$.

Recently Zhou et al. [22] proposed two classes of nonlinear feedback laws. The first one, consisting of nested saturation functions is a modification and generalization of the Teel's second type of nonlinear feedback law and the other one consists of parallel connections of saturation functions. Both these two types of nonlinear feedback laws need only $\tilde{n}$ saturation elements. Furthermore, the poles of the closed-loop system can be placed at any location of the left real axis when none of the saturation elements in the control laws is saturated.

Control Law 3 The first nonlinear feedback law proposed in [22] has the form

$$\tilde{\tau} = -\varepsilon_2 \sigma_1 \left(\left(\frac{\lambda_4 p_4 + \lambda_3 p_3}{\varepsilon_2} \right) + \frac{\varepsilon_1}{\varepsilon_2} \sigma_1 \left(\frac{\lambda_2 p_2 + \lambda_1 p_1}{\varepsilon_1} \right) \right) \tag{65}$$

where λ_i are tunable parameters, $\varepsilon_2 = 2 = \tilde{\tau}_{\max}$, $\varepsilon_1 = 0.4$ and the components of P have to be calculated using Eqs. 45–47 for given values of λ_i.

Control Law 4 The second control law proposed in [22] has the form

$$\tilde{\tau} = -\varepsilon_2 \sigma_1 \left(\frac{\lambda_4 p_4 + \lambda_3 p_3}{\varepsilon_2} \right) + \varepsilon_1 \sigma_1 \left(\frac{\lambda_2 p_2 + \lambda_1 p_1}{\varepsilon_1} \right) \tag{66}$$

where λ_i are tunable parameters, $\varepsilon_1 + \varepsilon_2 = 2 = \tilde{\tau}_{\max}$, $\varepsilon_1 = 0.4$ and the components of P have to be calculated using Eqs. 45–47 for given value of λ_i.

Control Law 5 This control law is proposed in [23] where the authors have extended the results given in [9]. The control law is in the form of

$$\tilde{\tau} = -\frac{\tilde{\tau}_{\max}}{\varepsilon^4 + \varepsilon^3 + \varepsilon^2 + \varepsilon} \sum_{i=1}^{4} \varepsilon^{4-i+1} \sigma_1 (p_i) \tag{67}$$

where $\lambda_i = \varepsilon^{4-i+1}$, $i = 1, 2, 3, 4$. ε has to satisfy the condition $\varepsilon \leq 0.5437$ to ensure stability and it is chosen in this investigation to be $\varepsilon = 0.5$. The components of P have to be calculated using Eqs. 45–47 for $\lambda_i = \varepsilon^{4-i+1}$; $\tilde{\tau}_{\max} = 2$.

4 Simulation Results

The control laws discussed in Section 3 have been compared by conducting autonomous flight simulations in Matlab–Simulink programming environment. An accurate dynamic model of the four rotor rotorcraft has been used. The model has been developed on the base of the Dragan-Flyer quad-rotor mini-rotorcraft flight dynamics presented in [32]. Its level of detail is greater compared to that of the model presented in Section 2 and subsequently used to design the stabilizing control schemes: rotor in-plane forces and moments, blade flapping dynamics and ground effect have been considered. The necessary experimental data have been obtained from wind tunnel tests. To model environmental conditions horizontal and vertical gusts have been also included. Thus the compared bounded feedback controllers have been required to handle the existing differences in the dynamic properties between the model described by the Eqs. 24–29 and this more accurate dynamic model.

During the simulations the control objective was to make the quad-rotor mini-rotorcraft to reach the position $(x, y, z) = (3, 3, 2)$ m while $(\psi, \theta, \phi) = (0, 0, 0)$ degrees. An initial mismatch of $\theta = -20°$ and $\phi = 20°$ is assumed. The gain values used for the altitude and yaw control laws are taken as $\alpha_{z1} = 0.8$, $\alpha_{z2} = 1$, $\alpha_{\psi 1} = 1$, $\alpha_{\psi 2} = 0.5$. The values of the parameters when Teel's first control law has been implemented for the pitch and roll control of the mini-rotorcraft have been chosen as $\alpha_1 = 2$, $\alpha_2 = 1$, $\alpha_3 = 0.2$, and $\alpha_4 = 0.1$ respectively. Series of experiments have been carried on in order to investigate the influence of the design parameters λ_i in the control laws 3–5 on the transient performance of the closed-loop system. Simulation results imply that $\lambda_1 = \lambda_2 = \lambda_3 = \lambda_4$ will lead to better transient performances. So in the following such a relation is assumed to be satisfied. Figures 3, 4, 5, 6, 7 and 8 show the comparison result in the case I when $\lambda_i = 0.5$ and Figs. 9, 10, 11, 12, 13 and 14 illustrate the comparison results in the case II when $\lambda_i = 0.9$.

The simulation results presented show that the two types of bounded feedback control laws proposed by Teel in [16] demonstrate different

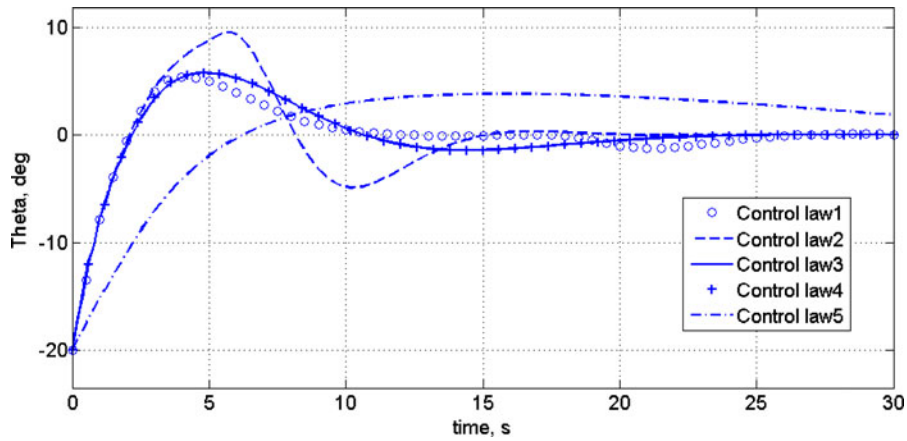

Fig. 3 Case I. Comparison result: the evolution of the pitch angle θ.

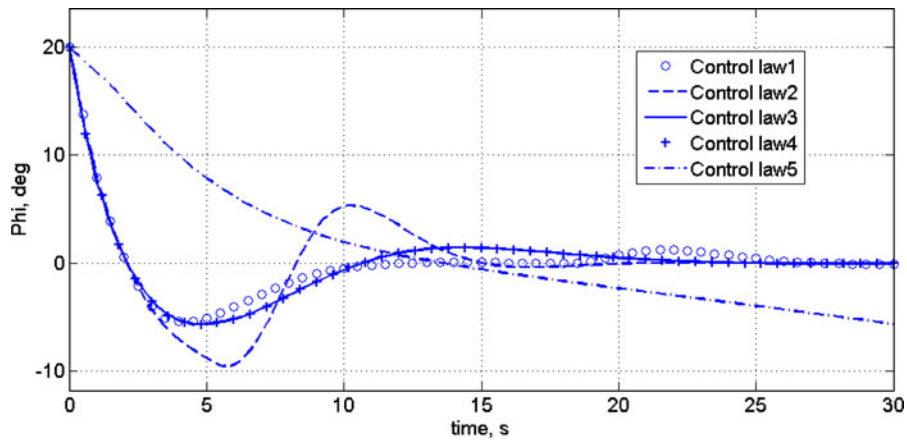

Fig. 4 Case I. Comparison result: the evolution of the roll angle ϕ

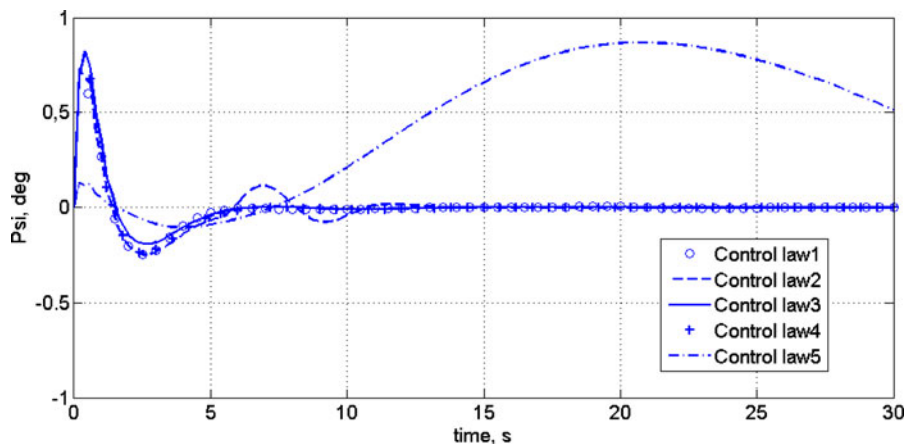

Fig. 5 Case I. Comparison result: the evolution of the yaw angle ψ

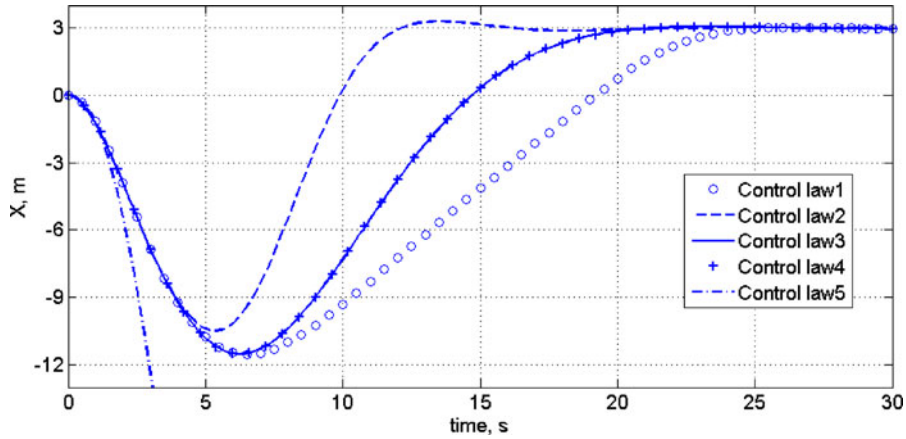

Fig. 6 Case I. Comparison result: the evolution of X coordinate

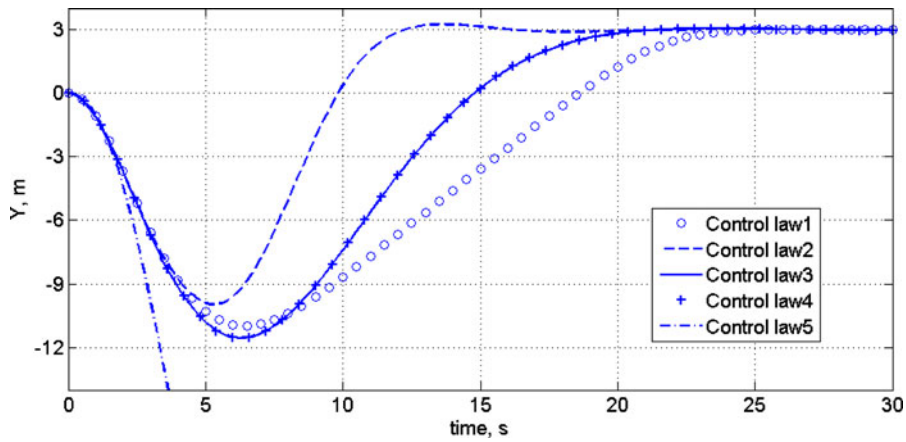

Fig. 7 Case I. Comparison result: the evolution of Y coordinate

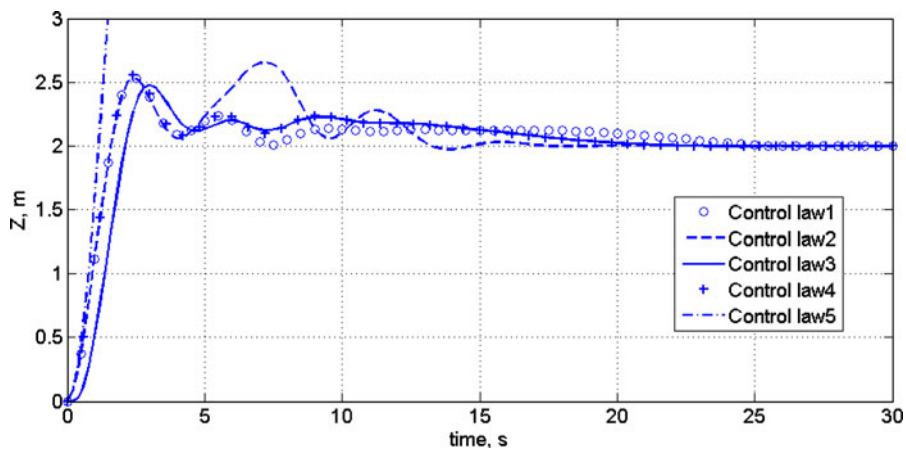

Fig. 8 Case I. Comparison result: the evolution of Z coordinate

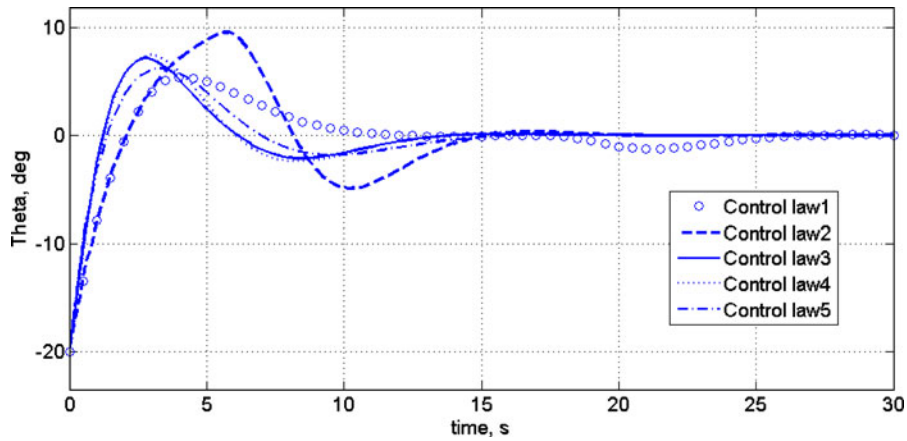

Fig. 9 Case II. Comparison result: the evolution of angle θ

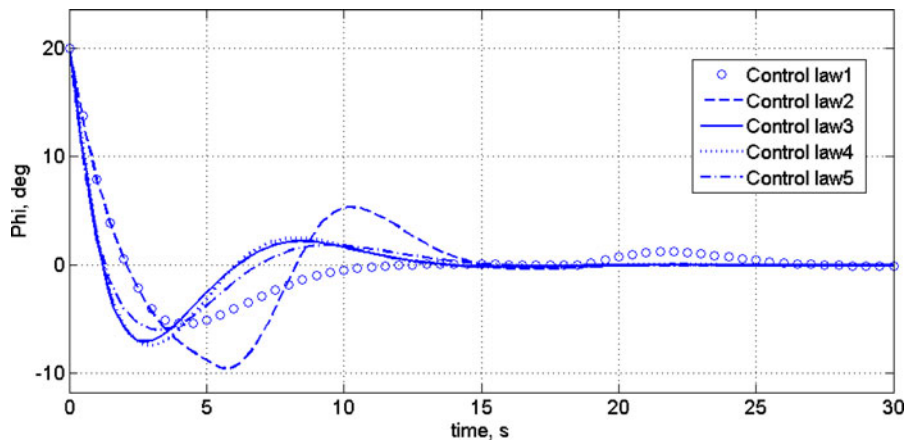

Fig. 10 Case II. Comparison result: the evolution of angle ϕ

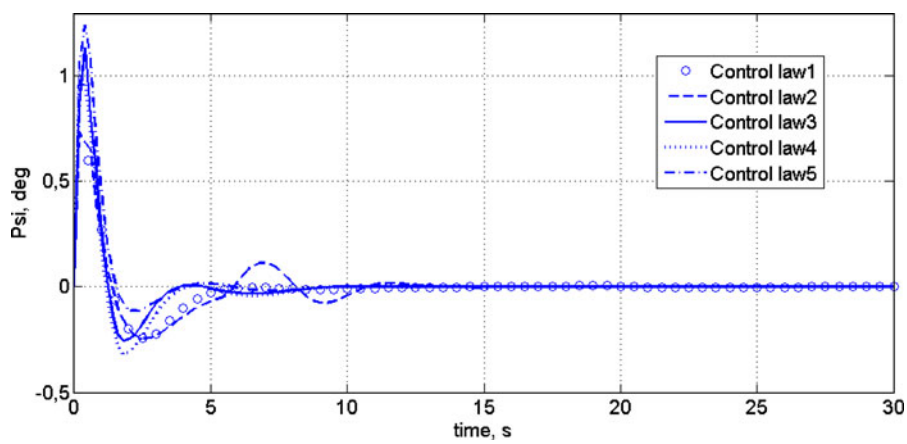

Fig. 11 Case II. Comparison result: the evolution of angle ψ

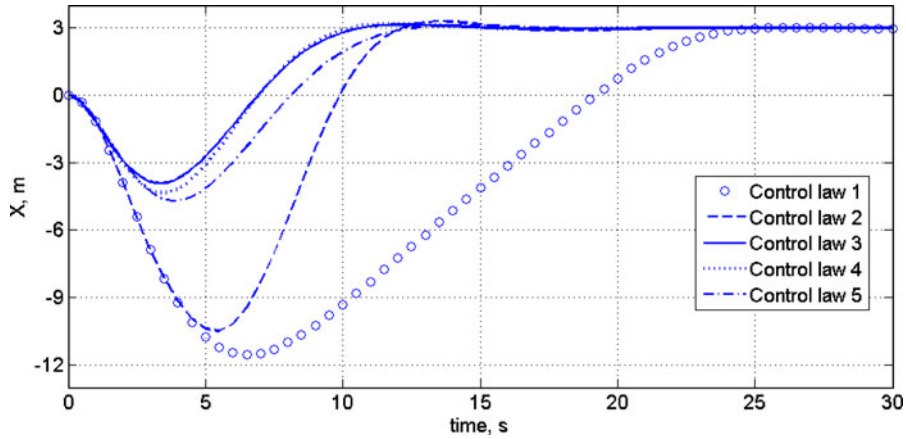

Fig. 12 Case II. Comparison result: the evolution of X coordinate

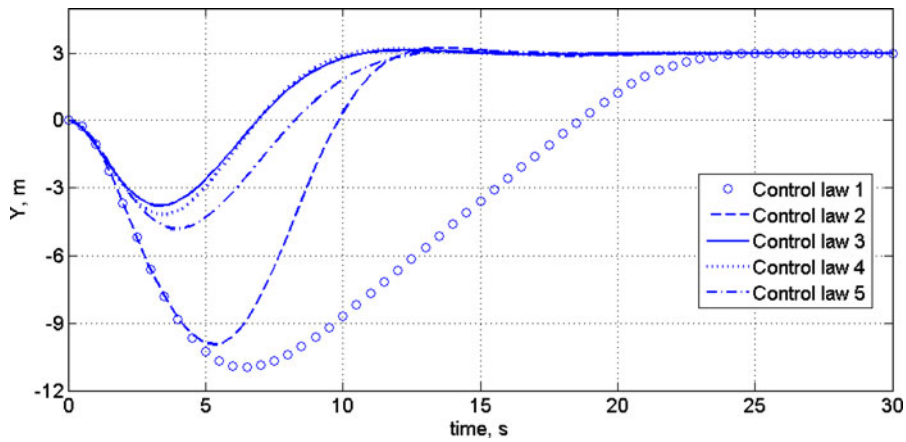

Fig. 13 Case II. Comparison result: the evolution of Y coordinate

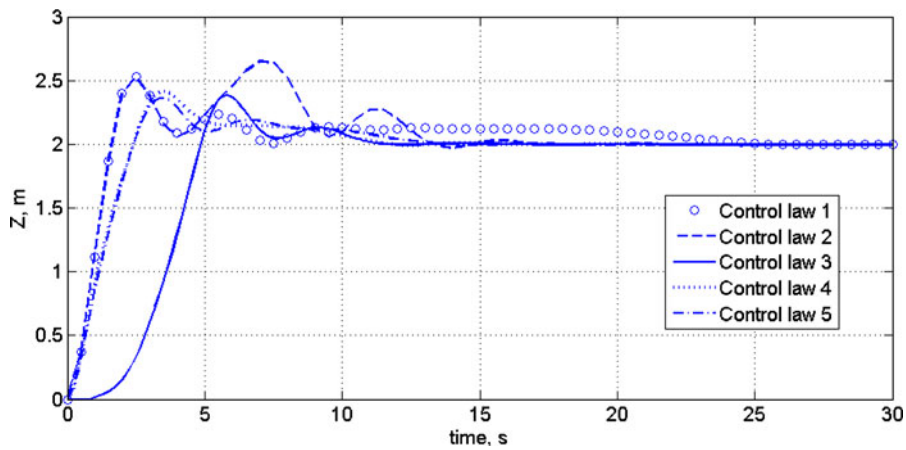

Fig. 14 Case II. Comparison result: the evolution of Z coordinate

performance, with the second control law showing better performance when the displacement along X and Y is considered while the first one stabilizes better pitch and roll angles. In addition the second control law is inherently superior to the first as it requires fewer saturation elements. The third and the fourth type of nonlinear control laws proposed by Zhou et al. in [22] require also fewer saturation elements and this simplifies the control strategy. This property is important in real-time applications. It can be observed from the simulations that the transient performance of the closed-loop system with control law 3 and control law 4 is almost identical with the control law 3 being slightly better than control law 4 in the case II (when $\lambda_i = 0.9$). Control law 5 does not work well in the case I (when $\lambda_i = 0.5$) while it gives similar results to control laws 3–4 in the case II (when $\lambda_i = 0.9$). With the decrease of λ_i the performance of the control laws 3–5 is rapidly deteriorating (see the comparison results in the case I when $\lambda_i = 0.5$). This contradicts to some extend to the results reported in [22, 23] where better closed loop performance is observed for smaller values of λ_i when the control laws 3–5 are applied for the global control of systems with multiple integrators. Our simulation experiments have shown that this is true when very big mismatch is assumed in the initial conditions for such systems. When the nested saturation control strategy is applied for stabilization of the quad-rotor rotorcraft however big initial mismatch in the initial values of the roll and pitch angles is not allowable because of the imposed upper bounds on $|\theta|$ and $|\phi|$ in order to assume $\sin(\theta) \approx \theta$ and $\sin(\phi) \approx \phi$.

5 Real-time Experimental Results

This section presents results from real-time autonomous flight experiments with the DraganFlyer V Ti miniature aerial vehicle manufactured by Draganfly Innovations Inc., (http://www.rctoys.com).

5.1 Hardware Setup

The experimental setup is composed of a DraganFlyer V Ti mini-rotorcraft, a four-channel GWS FM remote control radio unit, a Pentium IV PC with installed QuaRC 2.01 software for rapid prototyping from Quanser, and a 3-D tracker system (Polhemus Patriot), [33] used for measuring the position (X,Y,Z) and orientation (ϕ, θ, ψ) of the quadrotor.

The Polhemus Patriot system with an on-board position/orientation sensor is connected to the PC via RS 232 interface to allow feedback control (see Fig. 15). The PC generates control inputs, which are sent to the rotorcraft through the GWS radio control unit. The latter is connected to the computer via a Q4 Hardware-In-The-Loop board produced by Quanser. To simplify the experiments, each control input can be switched between automatic and manual control modes.

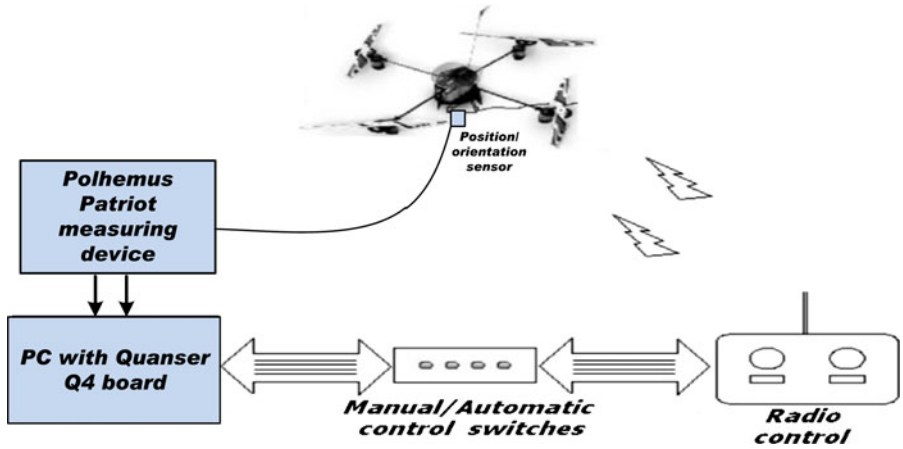

Fig. 15 The experimental setup

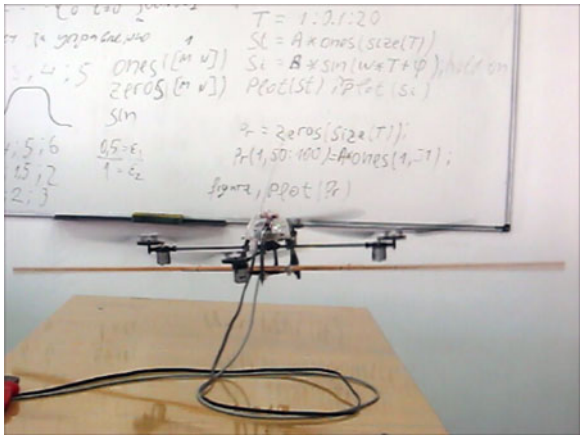

Fig. 16 A real-time control of the quad-rotor experimental platform in autonomous hover

Figure 16 shows the quad-rotor experimental platform in autonomous hover. The wires attached to the rotorcraft provide connections to the power supply and the position-attitude sensor. A wooden stick is attached to the rotorcraft for safety.

5.2 Experimental Tests

Since the third control law has shown the best overall performance during the conducted flight simulations (with $\lambda = 0.9$) it has been selected and further implemented in real-time for autonomous flight tests. The performance of the control algorithm has been evaluated in three experiments. The first and the second real-time experiments have been conducted by automatically controlling the quad-rotor rotorcraft in the vertical plane while manually keeping the roll and yaw angles close to zero. Thus the control of the rotorcraft has been reduced to a Planar Vertical Take-Off and Landing (PVTOL) aircraft control problem. During the third experiment a real-time control of the quad-rotor platform in autonomous hover has been attempted.

To stabilize the system, the tunable control gains (ε_1, ε_2) obtained from the simulations have been first implemented. Then they have been refined experimentally to $\varepsilon_2 = 0.5$, $\varepsilon_1 = 0.2$ for the pitch angle control channel and $\varepsilon_2 = 2$, $\varepsilon_1 = 0.6$ for the roll angle control channel. The different gains of the two control channels are probably due to the attached wooden stick (see Fig. 16). The discretization time has been set to 16 ms.

During the first experimental test the control objective has been defined to make the four-rotor mini-rotorcraft to reach a position $(X, Z) = (0, 15)$ cm in the vertical plane. An initial mismatch of $\theta = 6°$ and $X = 12$ cm has been introduced. The results are shown on Figs. 17, 18 and 19.

In the second experiment the rotorcraft has been expected to move horizontally 15 cm from an initial point with coordinates $(X, Z) = (0, 15)$ cm on the vertical plane to a new point with coordi-

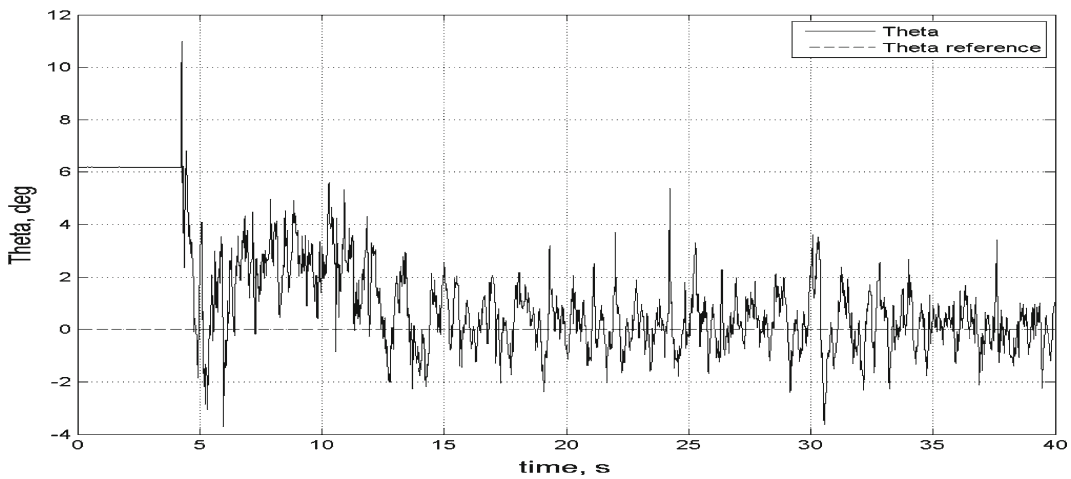

Fig. 17 Case I. PVTOL experiment with non-zero initial conditions: the evolution of angle θ

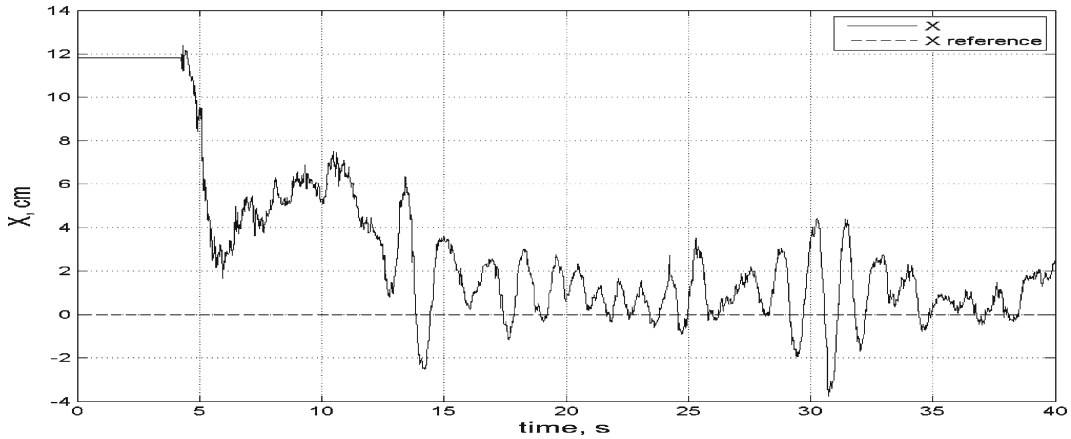

Fig. 18 Case I. PVTOL experiment with non-zero initial conditions: the evolution of X coordinate

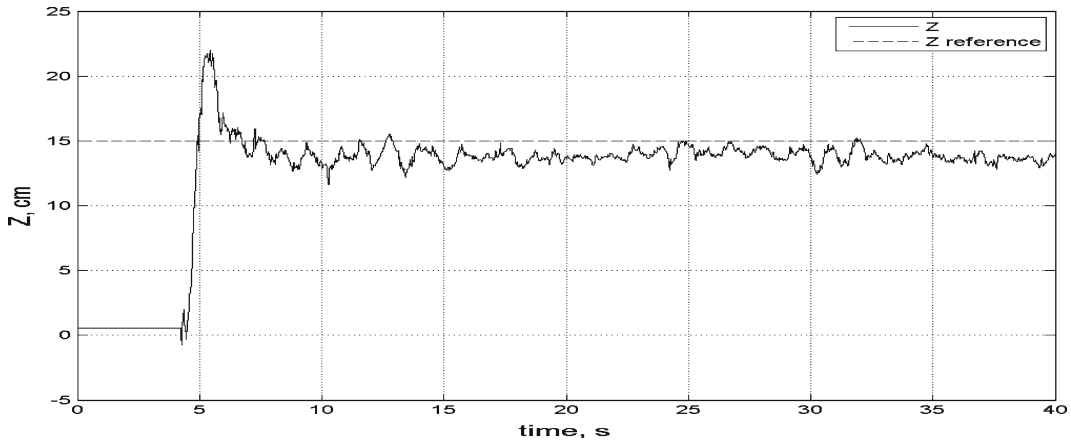

Fig. 19 Case I. PVTOL experiment with non-zero initial conditions: the evolution of Z coordinate

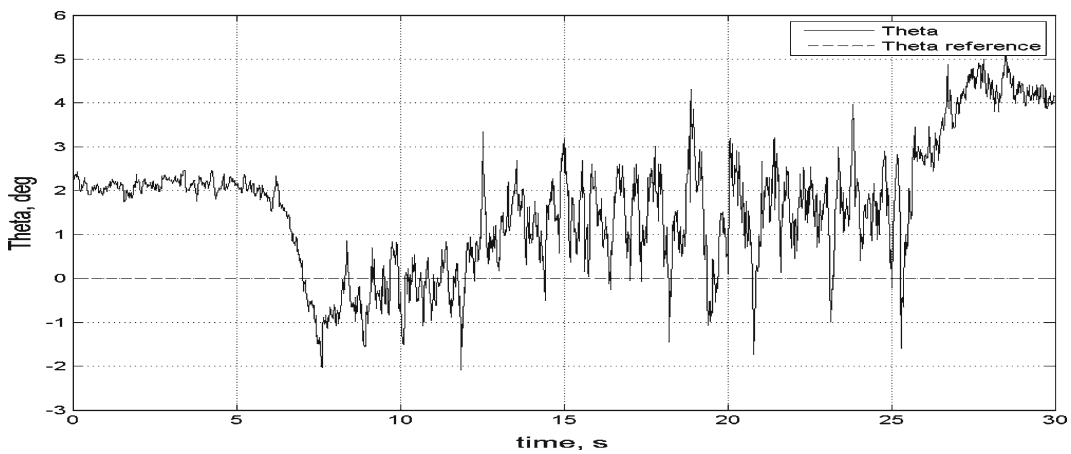

Fig. 20 Case II. PVTOL experiment with non-zero X reference: the evolution of angle θ

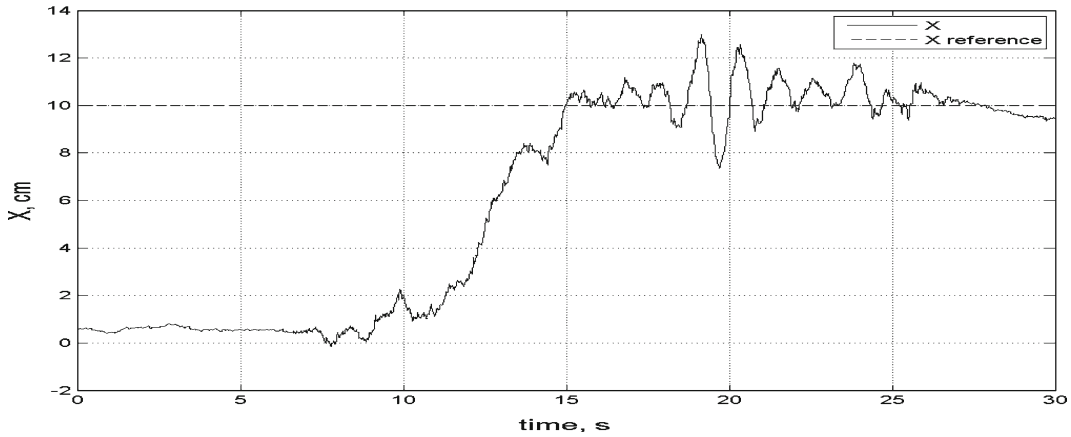

Fig. 21 Case II. PVTOL experiment with non-zero X reference: the evolution of X coordinate

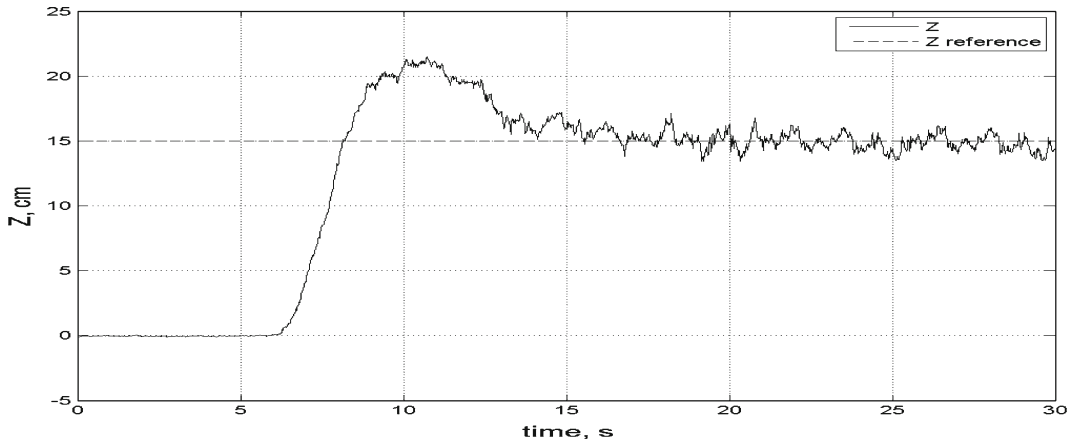

Fig. 22 Case II. PVTOL experiment with non-zero X reference: the evolution of Z coordinate

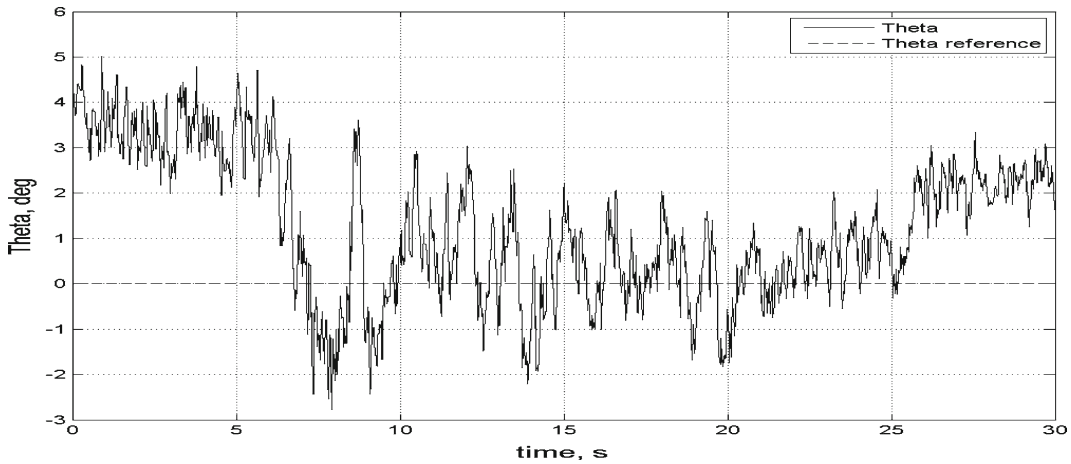

Fig. 23 Case III. The quadrotor autonomous hover experiment: the evolution of angle θ

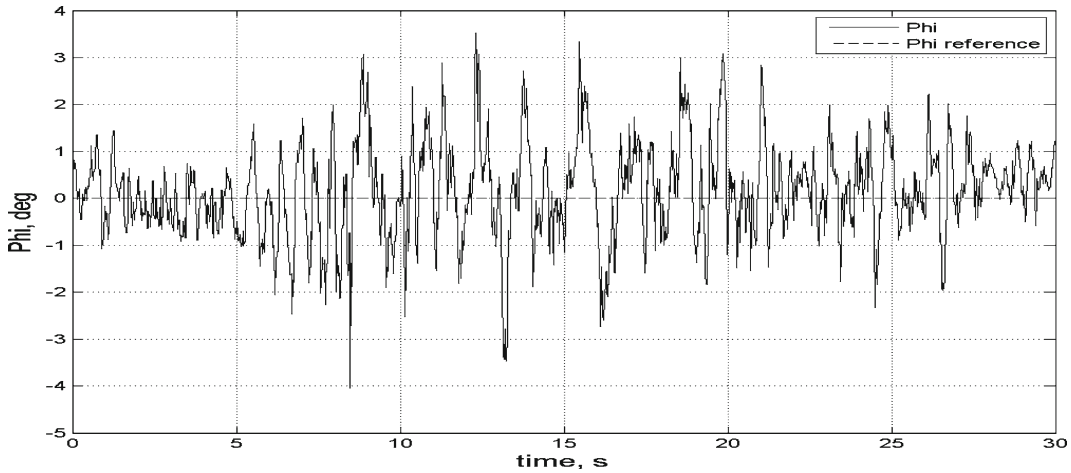

Fig. 24 Case III. The quadrotor autonomous hover experiment: the evolution of angle φ

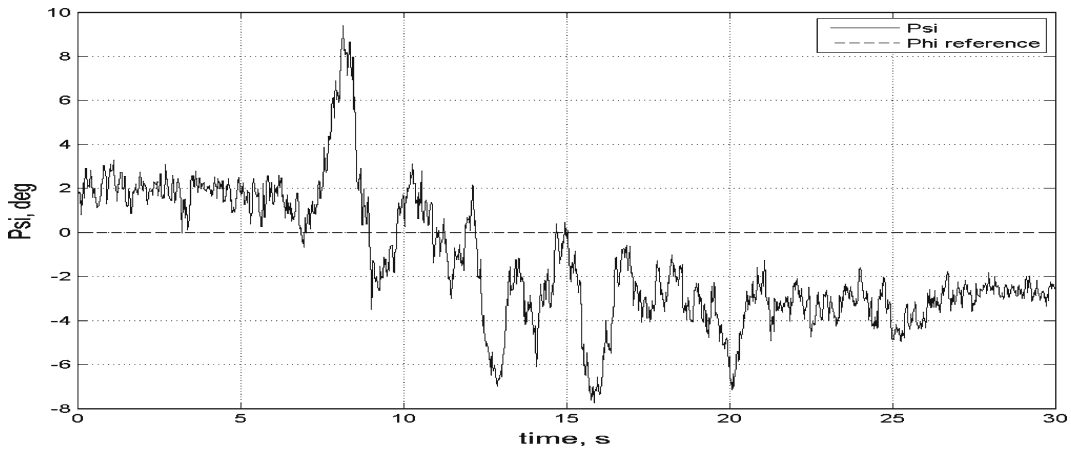

Fig. 25 Case III. The quadrotor autonomous hover experiment: the evolution of angle ψ

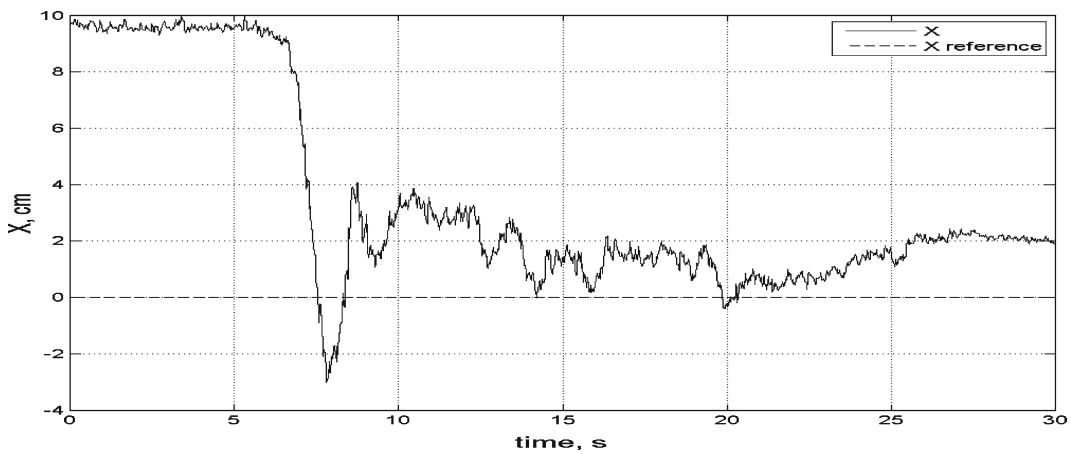

Fig. 26 Case III. The quadrotor autonomous hover experiment: the evolution of X coordinate

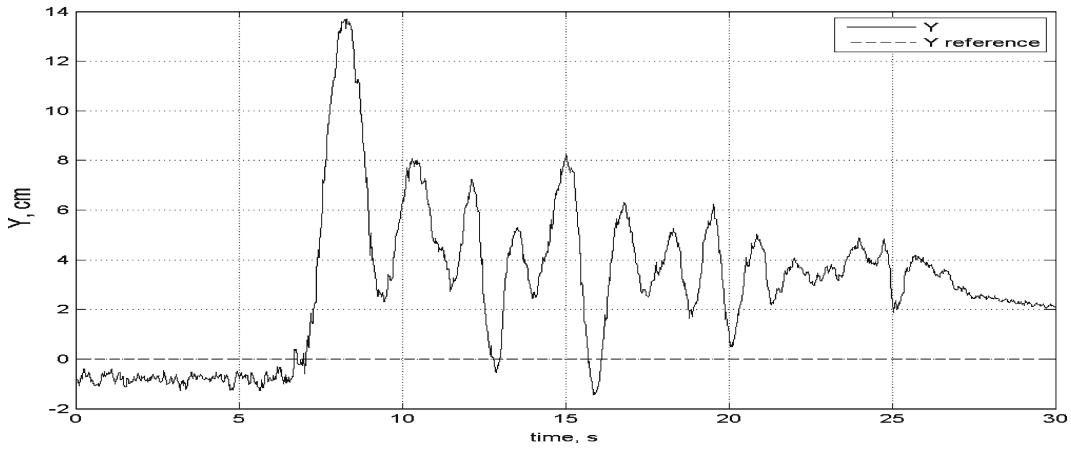

Fig. 27 Case III. Quadrotor autonomous hover experiment: the evolution of Y coordinate

nates $(X, Z) = (10, 15)$ cm. Figures 20, 21 and 22 show the performance of the control law 3 when applied to the mini-rotorcraft.

During the last experiment the rotorcraft has been placed in an arbitrary position, $(X, Y, Z) = (10, -1, 0)$ cm and the control objective has been defined to make the rotorcraft hover at an altitude of 25 cm, that is, to reach the position $(X, Y, Z) = (0, 0, 25)$ cm while $(\phi, \theta, \psi) = (0°, 0°, 0°)$. The obtained results are presented on Figs. 23, 24, 25, 26, 27 and 28.

It can be seen from the above experiments that during the first and second real-time flight tests the quad-rotor rotorcraft have been able to follow quite satisfactorily the desired reference. In the third experiment an existing gap between the real altitude of the rotorcraft and the desired altitude is shown on Fig. 28. The reference altitude in this experiment is higher than in the previous two experiments and most probably the existing gap indicates that the gains of the altitude controller need further tuning. The same is required also for rest of the tunable parameters in order to obtain a better performance. In another work the authors have proposed to implement on-line tuned neural networks for handling unknown nonlinearities and the obtained results from simulations have shown that this can significantly improve the performance of the quadrotor altitude and yaw controllers [7].

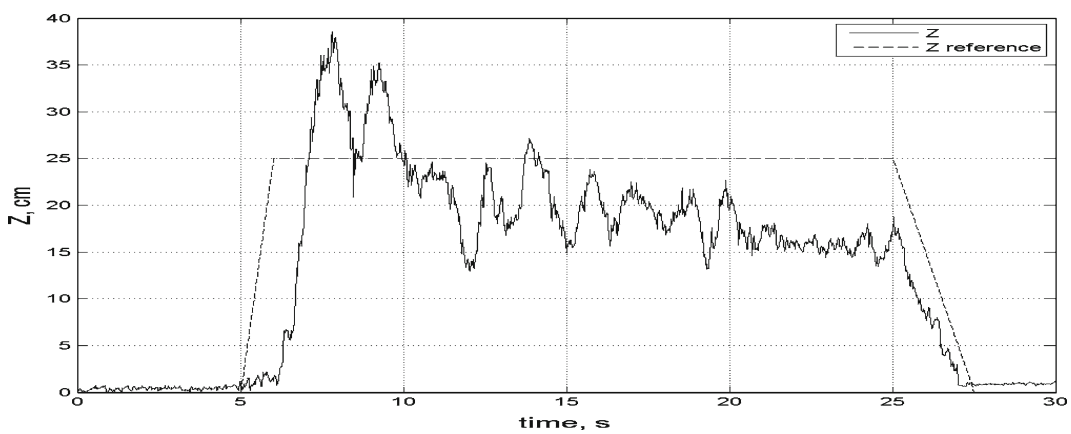

Fig. 28 Case III. The quadrotor autonomous hover experiment: the evolution of Z coordinate

6 Conclusion

In this investigation five different types of nonlinear feedback control laws with saturation elements, previously proposed for the global control of systems with multiple integrators, have been successfully applied and tested to control the DraganFlyer V Ti quad-rotor mini-rotorcraft roll and pitch angles during autonomous flights. The results obtained through simulations and real-time experiments have been analyzed with respect to the structural simplicity of the control schemes and the transient performance of the closed-loop system.

Acknowledgements The work of A. V. Topalov and N. G. Shakev was supported in part by the TU Sofia Research Fund Project 102ni083-19 and in part by the Ministry of Education, Youth and Science of Bulgaria Research Fund Project BY-TH-108/2005. The work of O. Kaynak was supported by the TUBITAK Project 107E248.

References

1. Bouabdallah, S., North, A., Siegwart, R.: PID vs LQ control techniques applied to an indoor micro quadrotor. In: Int. Conf. on Intelligent Robots and Systems, pp. 2451–2456 (2004)
2. Castillo, P., Lozano, R., Dzul, A.E.: Stabilization of a mini rotorcraft with four Rotors. IEEE Control Syst. Mag. **25**, 45–55 (2005)
3. Mokhtari, A., Benallegue, A., Daachi, B.: Robust feedback linearization and GH∞ controller for a quadrotor unmanned aerial vehicle. J. Electr. Eng. **57**(1), 20–27 (2006)
4. Yang, C.D., Liu, W.H.: Nonlinear H∞decoupling hover control of a helicopter with parameter uncertainties. In: Proc. American Control Conference. Denver, Colorado (2003)
5. Kim, H.J., Shim, D.H., Sastry, S.: Nonlinear model predictive tracking control for rotorcraft-based unmanned aerial vehicles. In: Proc. of the American Control Conference. Anchorage, AK (2002)
6. Das, A., Lewis, F., Subbarao, K.: Backstepping approach for controlling a quadrotor using Lagrange form dynamics. J. Intell. Robot. Syst. **56**, 127–151 (2009)
7. Topalov, A.V., Shakev, N.G., Kaynak, O., Kayacan, E.: Neuro-adaptive approach for controlling a quad-rotor helicopter using sliding mode learning algorithm. In: Proc. of the IFAC Int. Workshop on Adaptation and Learning in Control and Signal Processing ALCOSP-2010. Antalya, Turkey (2010)
8. Dornheim, M.A.: Report pinpoints factors leading to YF-22 crash. Aviat. Week Space Technol. **137**(19), 53–54 (1992)
9. Sussmann, H.J., Sontag, E.D., Yang, Y.: A general result on the stabilization of linear systems using bounded controls. IEEE Trans. Autom. Control **39**(12), 2411–2425 (1994)
10. Suarez, R., Alvarez-Ramirez, J., Solis-Daun, J.: Linear systems with bounded inputs: Global stabilization with eigenvalue placement. Int. J. Robust Nonlinear Control **7**(9), 835–846 (1997)
11. Lin, Z., Saberi, A.: Semi-global exponential stabilization of linear discrete-time systems subject to input saturation via linear feedback. Syst. Control Lett. **24**, 125–132 (1995)
12. Gomes da Silva, J.M. Jr., Tarbouriech, S.: Local stabilization of discrete time linear systems with saturating controls: An LMI-based approach. IEEE Trans. Autom. Control **46**(1), 119–124 (2001)
13. Hu, T., Lin, Z.: Exact characterization of invariant ellipsoids for single input linear systems subject to actuator saturation. IEEE Trans. Autom. Control **47**(1), 164–169 (2002)
14. Liu, W., Chitour, Y., Sontag, E.: On finite gain stabilizability of linear systems subject to input saturation. SIAM J. Control Optim. **34**, 1190–1219 (1996)
15. Saberi, A., Lin, Z., Teel, A.R.: Control of linear systems with saturating actuators. IEEE Trans. Autom. Control **41**(30), 368–378 (1996)
16. Teel, A.R.: Global stabilization and restricted tracking for multiple integrators with bounded controls. Syst. Control Lett. **18**(3), 165–171 (1992)
17. Castillo, P., Lozano R., Dzul, A.E.: Modelling and Control of Mini-Flying Machines. Springer, London (2005)
18. Castillo, P., Lozano R., Dzul, A.E.: Real-time stabilization and tracking of a four-rotor mini rotorcraft. IEEE Trans. Control Syst. Technol. **12**(4), 510–516 (2004)
19. Rao, V.G., Berstein, D.S.: Naive control of the double integrator. IEEE Trans. Control Syst. Mag. **21**(5), 86–97 (2001)
20. Marchand, N.: Further results on global stabilization for multiple integrators with bounded controls. In: Proc. of the 42nd IEEE Conference on Decision and Control, pp. 4440–4444. Maui, Hawaii USA (2003)
21. Johnson, E.N., Kannan, S.K.: Nested saturation with guaranteed real poles. In: Proceedings of the American Control Conference 1, pp. 497–502 (2003)
22. Zhou, B., Duan, G.-R., Li, Z.-Y.: On improving transient performance in global control of multiple integrators system by bounded feedback. Syst. Control Lett. **57**, 867–875 (2008)
23. Marchand, N., Hably, A.: Global stabilization of multiple integrators with bounded control. Automatica **41**, 2147–2152 (2005)
24. Marchand, N., Hably, A., Chemori, A.: Global stabilization with low computational cost of the discrete-time chain of integrators by means of bounded controls. IEEE Trans. Autom. Control **52**(5), 948–952 (2007)

25. Kannan, S.K., Johnson, E.N.: Adaptive control with a nested saturation reference model. In: Proceedings of the AIAA Guidance, Navigation and Control Conference, pp. 1–11. Austin, TX (2003)
26. Zhu, K., Krishnan, S.M.: Stabilization of discrete-time multi-integral systems with input constraint. In: Proceedings of the 36nd IEEE Conference on Decision and Control, San Diego, California, USA pp. 4524–4528 (1997)
27. Lozano, R., Dimogianopoulos, D.: Stabilization of a chain of integrators with nonlinear perturbations: applications to the inverted pendulum. In: Proceedings of the 42nd IEEE Conference on Decision and Control, Maui, Hawaii USA pp. 5191–5196 (2003)
28. Marchand, N., Hably. A.: Improving the performance of nonlinear stabilization of multiple integrators with bounded controls. In: Proceedings of the IFAC World Congress (2005)
29. Hably, A., Kendoul, F., Marchand, N., Castillo, P.: Positive Systems. Lecture Notes in Control and Information Sciences, vol. 341. Chapter Further results on global stabilization of the PVTOL aircraft, pp. 303–310. Springer (2006)
30. Hably A., Marchand, N.: Global stabilization of four-rotor helicopter with bounded inputs. In: Proceedings of IEEE/RSJ Int. Conf. on Intelligent Robots and Systems (IROS), pp. 129–134 (2007)
31. Craig, J.J.: Introduction to Robotics: mechanics and control, 3rd edn. Pearson Education, Inc., Prentice Hall (2005)
32. Martinez, V.: Modelling of the Flight Dynamics of a Quadrotor Helicopter. MSc thesis, Dept. of Aerospace Sciences, School of Engineering, Cranfield University, UK https://aerade.cranfield.ac.uk/handle/1826/2957 (2007)
33. Patriot User Manual, URM03PH170 Rev. E, Alken, Inc., dba Polhemus, Colchester, Vermont, USA (2008)